Electronic Structure of Cob(I)alamin: The Story of an Unusual Nucleophile

Kasper P. Jensen*

Department of Chemistry, Yale University, New Haven, Connecticut 06511

Received: February 15, 2005; In Final Form: March 24, 2005

The electronic structure and the ligand-field spectrum of cobalt(I) corrin is reported using complete active space multiconfigurational perturbation theory (CASPT2) to address some inconsistencies and the nature of the cobalt(I) "supernucleophile", cob(I)alamin. An assignment of six of the seven intense lines in the experimental spectrum is obtained at a root-mean-square accuracy of 0.14 eV and largest error of 0.21 eV. Agreement is significantly better for CASPT2 than density functional theory (DFT), but DFT does surprisingly well. The correlated wave function implies that the ground state of Co^I corrin is severely multiconfigurational, with only 67% of the d^8 reference configuration and prominent contributions of 20% from open-shell metal-to-ligand charge-transfer configurations. The ground state exhibits a fascinating degree of covalency between cobalt and the nitrogen orbitals, described by the bonding and antibonding orbital pair of a cobalt d-orbital and a δ-orbital linearly combined from nitrogen orbitals. Thus, the standard description of the d^8 supernucleophile is not completely valid. From a biological perspective, the mixing in of Co^{II} configurations in cob(I)alamin may be an important reason for the redox accessibility of the formal Co^I state of the cofactor, which again provides the catalytic power for one half-reaction of enzymes such as cobalamin-dependent methionine synthase.

Introduction

Cobalamins constitute a unique group of cobalt complexes functioning as cofactors for a variety of enzymes, in particular mutases and transferases. Humans utilize one of each of these classes, namely, methionine synthase (MES) and methylmalonyl coenzyme A mutase (MCAM).[1] As seen in Figure 1, the cobalamin skeleton is quite complex, consisting of a central monoanionic corrin ring with 13 conjugated atoms, including 14 π-electrons. In the center of the corrin ring, a cobalt ion is found. The coenzyme is digested as vitamin B$_{12}$ (cyanocobalamin) with the upper axial ligand (R) being CN$^-$. The vitamin is subsequently converted into two active forms of the coenzyme in the body; the nature of the R group is changed, MCAM uses 5′-deoxyadenosylcobalamin whereas MES uses methylcobalamin. The organometallic Co−C bond, which is broken during catalysis, is a unique entity in biology, and understanding the reactivity of this bond has been a major subject of research within the field of bioinorganic chemistry.[1]

The cobalamins are capable of sustaining cobalt in three oxidation states, III, II, and I, with the latter being very uncommon due to its unfavorable redox potential. However, in methyl transferases, a remarkable 4-coordinate cob(I)alamin intermediate is the active species that presumably attacks 5-methyltetrahydrofolate and forms the Co^{III}−methylcobalamin while recycling tetrahydrofolate in the folate cycle (Figure 2).[2,3] Homocysteinate then attacks methylcobalamin and is methylated by heterolytic cleavage of the Co−C bond into methionine, leaving cob(I)alamin.[4,5] Thus, two highly nucleophilic[6] species are the central players in this "ping pong"[5] S$_N$2 reaction. A porphyrin ring, which is dianionic, cannot accomplish the feat of stabilizing the monovalent oxidation state in heme proteins[7] but has accessible high-valent states such as Fe^{IV}.

Figure 1. Cobalamin skeleton.

The power of such a strong cob(I)alamin nucleophile has been attributed to the two electrons occupying the axial d$_{z^2}$ orbital (Figure 3). The species is electron paramagnetic resonance

---

* Author to whom correspondence should be addressed. E-mail: kasper.jensen@yale.edu.
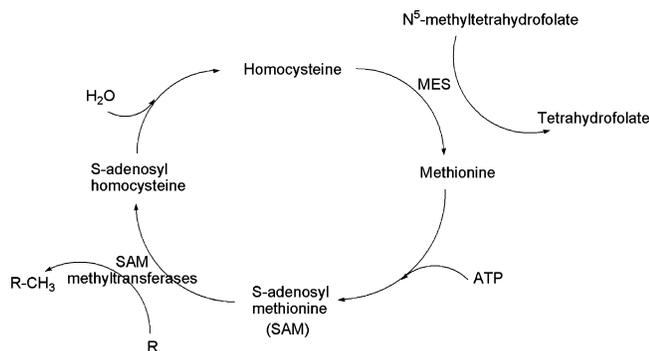
Figure 2. Function of methionine synthase (MES) in methylation pathways.
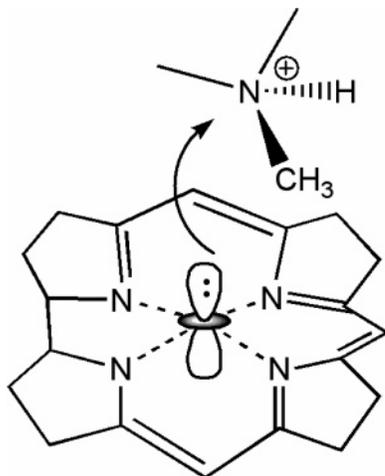
Figure 3. Function of d[8] Co[I] corrin as a supernucleophile in methyl transfer.

(EPR) silent, suggesting a low-spin singlet ground state. Indeed, cobalamin chemistry is low-spin chemistry, an observation that was recently rationalized from specific properties of cobalt and the size of the corrin ring cavity.[7] Naturally, one would assume, as has been done hitherto, a single configuration wave function with doubly occupied d_{xy}, d_{xz}, d_{yz}, and d_{z^2} orbitals to satisfactorily describe this molecule. For the standard cobalt(I) corrin model, shown in Figure 4, this would (in C_2 symmetry) correspond to a ^1A ground state. However, a singlet instability in the restricted wave function description was recently puzzling, with density functional theory (DFT) giving an open-shell singlet at 4 kJ/mol lower energy than the restricted Kohn−Sham solution.[7] This could be a sign of a more complex wave function of cob(I)-alamin than first meets the eye, and thus the aim is to access in detail the electronic nature of this "supernucleophile" of cobalamin chemistry.

All recent theoretical work on cobalamins that has been performed in the new millennium can be called the "DFT + corrin" paradigm and has provided an excellent description of geometries,[7−13] however, with some problems (and solutions) describing other properties such as the essential Co−C bond strength.[14,15] Recent studies have also dealt with the electronic and vibrational spectra of some corrins, obtained from semi-empirical methods or time-dependent DFT, assuming closed-shell monoconfigurational wave functions.[16−18] In particular, the importance of the electronic structure and spectrum of the cob(I)alamin has already led to a computational study[18] of the model complex in Figure 4, cobalt(I) corrin.

In this work, the electronic structure and spectrum of Co[I] corrin is reported using a state-of-the-art *ab initio* method for electronic spectra together with multireference configurational
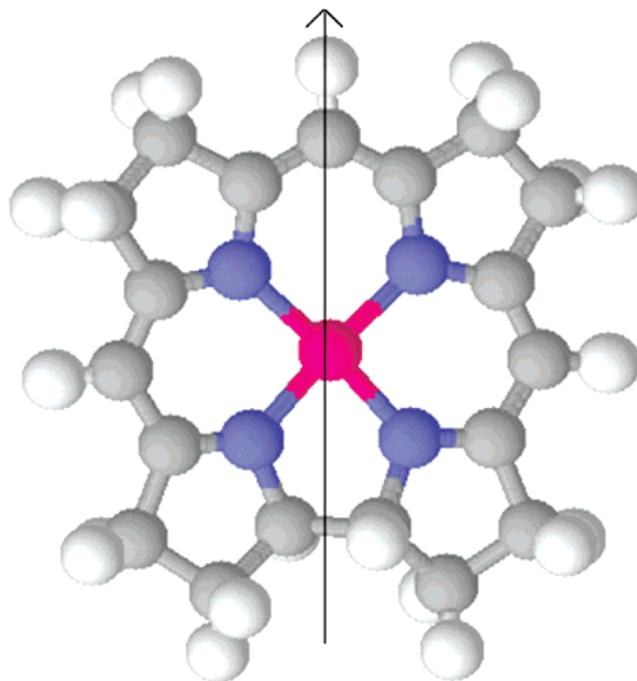
Figure 4. Optimized geometry of the cob(I)alamin model, cobalt(I) corrin, and C_2 axis of symmetry. The *x*- and *y*-axes are defined as intersecting the nitrogen atoms.

interaction (CI), complete active space second-order perturbation theory (CASPT2). Except for some monoconfigurational Møller−Plesset second-order (MP2) perturbation theory geometry optimizations,[14] this is the first ab initio treatment of an electronic problem involving the entire corrin ring. The method takes into account both nondynamical and dynamical correlation energy, in contrast to normal MP2, which is unable to treat the near-degeneracy effects of metal complexes. The most important finding is that the standard description of the d[8] supernucleophile is not completely valid. The reference configurational state function (HF wave function) accounts for $^2/_3$ of the wave function, but Co 3d $\rightarrow$ corrin π metal-to-ligand charge transfer (MLCT) makes up 23% of the ground state, in accordance with the open-shell singlet earlier obtained from DFT.[2] Whereas the first excited states of each symmetry, $^1A(2)$ and $^1B(1)$, are almost completely monoconfigurational, all other excited states should preferably be described in terms of mixtures of various configurations involving many double excitations and MLCT excitations.

Methods

Model Systems. The chemical model that includes the corrin ring (Figure 4) is considered a realistic model of cobalamins[19] and is confirmed by the accuracy of the results presented here. The structure of the complex was optimized at the unrestricted B3LYP level with the 6-31G(d) basis set.[20] This structure, which has been described before,[7] is very close to experiment (~0.02 Å in Co−N bond lengths). Turbomole,[21] version 5.6, was used for this task. The application of C_2 symmetry was initially thought to be a significant constraint, but subsequent comparison of C_1 and C_2 structures (Table 1) showed that only small changes occurred in the distant torsion angles. The corrin fold angles differed by ~0.4°. All bond lengths, including the Co−N distances ($\Delta r \approx 0.0002$ Å), and through-space distance from Co to the nearest carbon ($\Delta r \approx 0.002$ Å) were unaffected by the symmetry constraint. Any distortion is minimal, so the

Electronic Structure of Cob(I)alamin

J. Phys. Chem. B, Vol. 109, No. 20, 2005 **10507**

TABLE 1: B3LYP Results with C_2 Restricted and Unsymmetrical C_1 Corrin Models: Equatorial Co–N Distances, Distance to Nearest Carbon, Total Electronic Energy, and Corrin Fold Angle

	Co–N1 (Å)	Co–N2 (Å)	Co–C (Å)	energy (au)	fold angle (deg)
C_1	1.912	1.852	2.842	−2337.87339	5.8
C_2	1.911	1.852	2.840	−2337.87338	6.1

isolated corrin ring is, in all respects, effectively of C_2 symmetry. This is also seen in the computed B3LYP energies, which are identical to within 10^{-5} hartree. It is thus also adequate, in more general cases, to describe the isolated corrin ring as C_2 symmetric.

Computation of the spectrum was done with the MOLCAS 6.0 software,[22] which includes the state-of-the-art implementation of CASPT2 for calculating accurate excitation energies of multiconfigurational wave functions.[23−25] The basis set used was the ANO-S basis set.[26] The number of contracted basis functions were for Co, [5s4p3d1f], for N, [3s2p1d], for C, [3s2p], and for H, [2s]. This was the computationally largest possible basis set that still included a balanced treatment of correlation and polarization effects in Co and N atoms.

Determination of Reference Wave Function and Active Space. The Hartree−Fock self-consistent field (HF-SCF) reference wave function was calculated from the Aufbau procedure in MOLCAS, with a double occupation of 50 a and 45 b orbitals, in accordance with DFT. This dominant ground state d^8 configuration is supposed to have only the $d_{x^2−y^2}$ orbital empty and the 4 other d-orbitals doubly occupied when the z-axis is taken as the normal vector to the corrin ring plane (the C_2 axis is the between the x- and y-axes). To finish the d-shell and to include the double-shell effect, 6 + 4 orbitals with partial d-character orbitals were included in the active space, as seen in Figure 5 (48−50a, 52−54a, 44−47b). To secure saturation of the active space, the influence of several orbitals aside from the 10 electrons in 6 + 4 active d-orbitals was then evaluated. An extra orbital from the corrin ring of a symmetry (51a) was included, obtained as the lowest unoccupied linear combination of the nitrogen π-orbitals. An orbital with nitrogen σ-character in the active space was also included, but in the final optimized active space shown in Figure 5, this orbital mixed with the d-orbital to give 44b, which is seen to include both $d_{x^2−y^2}$ and nitrogen σ-character, and it is doubly occupied, so it is well-described in the already mentioned 10 orbitals with d-character. In fact, 44b and 46b form the important bonding−antibonding
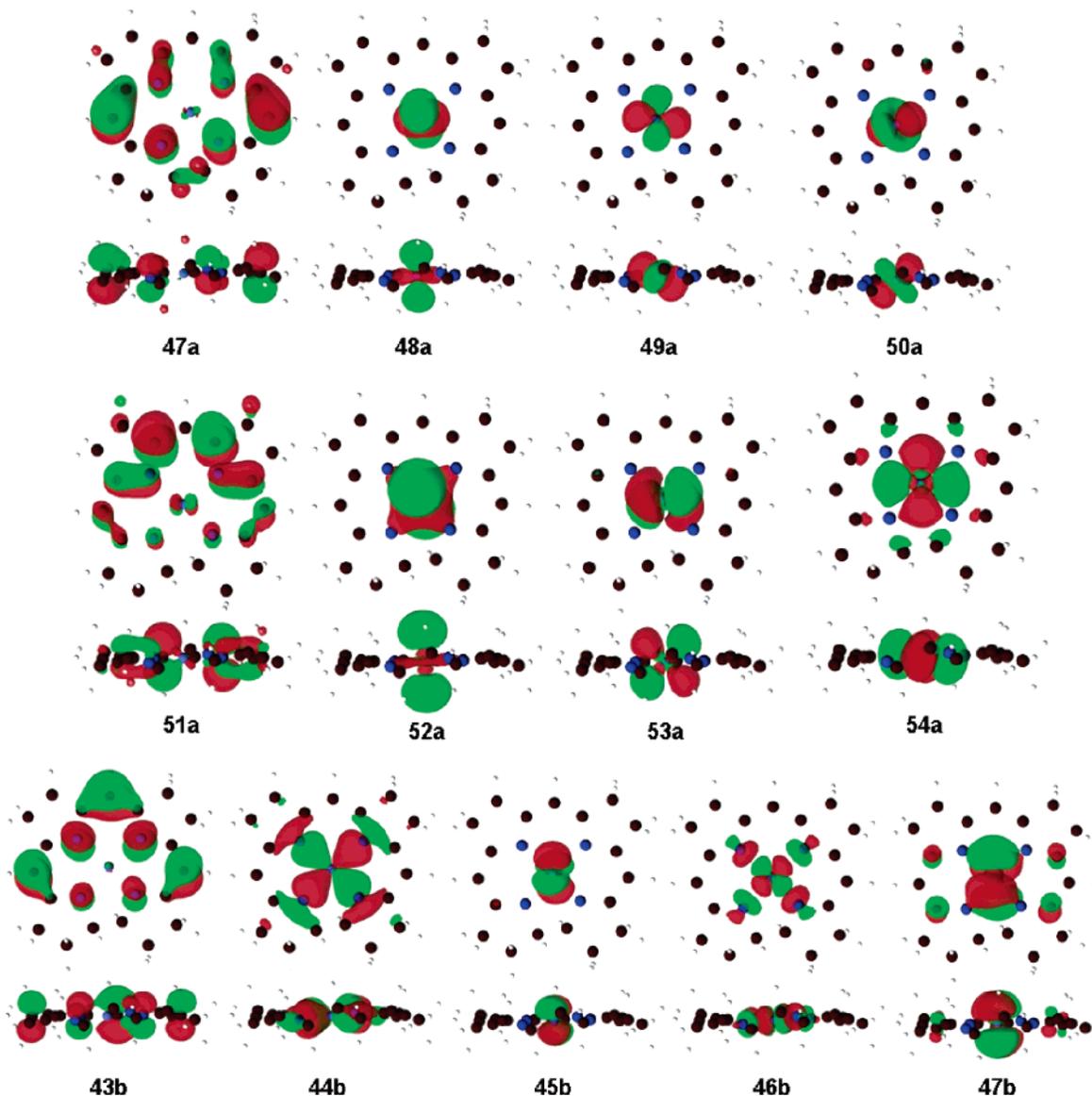
Figure 5. Molecular orbitals of active space and highest occupied inactives (47a and 43b), ^{1}A state.

TABLE 2: Composition of Active Space in Terms of Most Important Atomic Components of MOs[a]

MO	main AO	MO	main AO
a48	**Co 3d$_{z^2}$**	**b44**	**Co 3d$_{x^2-y^2}$ − N σ***
a49	**Co 3d$_{xy}$ (distorted)**	**b45**	**3d$_{yz}$**
a50	**Co 3d$_{xz}$ − 3d$_{z^2}$ (distorted)**	**b46**	**N σ* + Co 3d$_{x^2-y^2}$**
a51	corrin π	b47	Co 4d$_{yz}$
a52	Co 4d$_{z^2}$		
a53	Co 4d(xz)		
a54	Co 4d$_{xy}$		

[a] Boldface indicates occupied in the reference wave function.
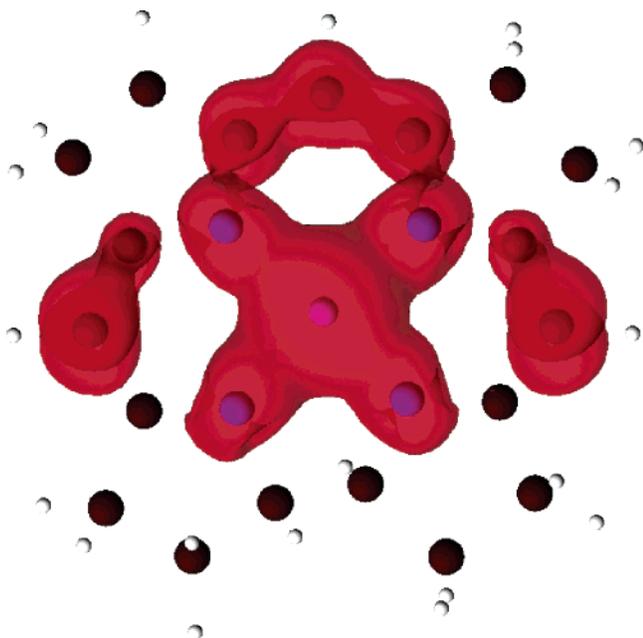
Figure 6. Partial density plot of active orbitals. The figure shows the full CI-correlated part of the electron density.

orbital set for this interesting covalent interaction, which shall be discussed later. Thus, charge transfer between ring and metal, as was anticipated to be of importance, is included via 51a, 44b, and 46b. This finally gave the used 10 electrons in a (7 + 4) active space, as described in Table 2. The density of this active space is depicted in Figure 6, describing the part of the molecule's electron density which is correlated at the CI level (other parts, in particular the core densities, are correlated at the MP2 level).

The inclusion of several other orbitals was also tested, including a charge-transfer orbital of b symmetry, (6 + 5), and larger spaces. These were similar or inferior to the (10 electrons in 7 + 4) space, and it was concluded that the (7 + 4) active space is saturated. All of the optimized molecular orbitals (MOs) have some d-character, with that of 51a being very small. A direct correlating orbital to 51a, which attains significant occupation in the complete active space (CAS) wave functions, could ideally be included. However, when the active space was designed, it was as always done to obtain the smallest effective active space, due to computational limits. First of all, 47a is always doubly occupied when it appears in various test active spaces. The current space had no intruder states, and all excited states were well-described even though the contribution from 51a changes, as also witnessed by the good excitation energies.

Computational Details. The CAS-SCF[27] wave function is used in CASPT2 as a reference to determine the first-order wave function and the second-order energy.[23−25] This procedure is similar to MP2 using a CAS-SCF instead of a SCF reference wave function. The CAS-SCF wave function captures the major

part of the nondynamical correlation energy by mixing *configurations* at the full CI level in the active space. The number of interacting CI roots were 10 for all states. No orbitals were frozen in the calculations. The total CI space consisted of 106 772 Slater determinants. For [1]A states, this reduced to 30 592 CSFs in the actual calculation, whereas for the [1]B-states the final CI space included 30 392 CFSs.

The second-order perturbation treatment was carried out using the multistate (MS) CASPT2 method,[28] in which the space spanned by the state-average terms is subject to a perturbative Hamiltonian, where the diagonal elements correspond to the normal CASPT2 energies and the off-diagonal coupling elements represent the interaction under the influence of dynamic correlation. With diagonalization of this matrix, the MS-CASPT2 approach provides an adequate description in cases where the CAS-SCF wave function is not in itself a suitable reference or where a strong mixing occurs between the reference state and CAS-CI states. The weight of the reference function for the excited states must be very close to that for the ground state, since the MS-CASPT2 approach is sensitive to the good convergence of the CAS-SCF wave function and to the absence of intruder states. The reference weights of all the perturbatively modified states (0.56−0.57) were very similar, implying that the MS-CASPT2 description is valid. A level shift of 0.3 was applied to reduce the influence of intruder states. This is known not to affect the accuracy of CASPT2, which is ~0.3 eV for excitation energies when a saturated active space and a reasonable basis set is applied.[29]

Results and Discussion

Ground-State Electronic Structure of Co[I] Corrin. The optimized active space shown in Figure 5 deviates somewhat from simple ligand-field considerations. The nature of the CAS-SCF wave function is discussed here, which includes orbitals optimized specifically for the ground state (in contrast to the state-average wave function, which is optimized as a mixture of CI roots with similar weights). The active space has been chosen to describe the ligand field, i.e., the electronic structure of cobalt(I) and its immediate surroundings. However, the lowest unoccupied corrin-based MOs of π- and σ-nature have also been included into the optimized active space, to probe for communication between the tetrapyrrole ring and the metal ion. Among these orbitals are 51a (the corrin ring lowest unoccupied molecular orbital (LUMO) of π-symmetry) and 44b + 46b (a combination of d$_{x^2-y^2}$ and nitrogen σ-orbitals).

In a recent investigation,[30] it was shown using multistate CASPT2 that for the oxygen adduct of a realistic model of oxyheme, the traditional Gouterman orbital description[31] was unimportant for the electronic structure, including the description of the ligand-field spectrum. This result suggests that only particular oxidation states and choices of axial ligands facilitate communication between the tetrapyrrole ring and the metal (communication here means nondynamical correlation by display of configurations with both ring and metal character, in terms of covalent or ionic (charge-transfer) configurations). More specifically, the energies of the MOs with metal d-orbital character should be similar to those with ligand character to facilitate communication (as interaction is inversely proportional to the energy separation). This can be accomplished by changing the oxidation state (increasing oxidation state will lower the energies of the d-orbitals) or by changing the nature of the axial ligands.

Communication as defined above may be a very important feature for the biochemical functionality of the tetrapyrroles.

Electronic Structure of Cob(I)alamin

J. Phys. Chem. B, Vol. 109, No. 20, 2005 **10509**

TABLE 3: Composition of the CAS-CI Wave Functions of the Singlet States in Terms of the Three Major Configuration State Functions[a]

state	$E_{MS\text{-}CASPT2}$	CSF1 (weight)	CSF2 (weight)	CSF3 (weight)
$^1A(1)$	0.00	2220000 2200 (67%)	22ud000 2200 (20%)	2u2d000 2200 (3%)
$^1A(2)$	1.14	u22d000 2200 (91%)	2u2d000 2200 (3%)	u22d000 2020 (0%)
$^1B(1)$	1.55	222u000 20d0 (87%)	2u22000 20d0 (4%)	2uud000 2d20 (2%)
$^1A(3)$	1.81	22ud000 2200 (42%)	2u2d000 2200 (26%)	2220000 2200 (19%)
$^1A(4)$	2.13	2u2d000 2200 (51%)	22ud000 2200 (23%)	22ud000 2ud0 (9%)
$^1B(2)$	3.22	202u000 2d20 (27%)	uu2d000 2d20 (16%)	2u20000 2d20 (13%)
$^1B(3)$	3.28	202u000 2d20 (22%)	u220000 2d20 (17%)	uu2d000 2d20 (17%)
$^1A(5)$	3.36	22ud000 2ud0 (49%)	2220000 2ud0 (24%)	2u2d000 2ud0 (7%)
$^1B(4)$	3.68	u2ud000 2d20 (62%)	22u0000 2d20 (7%)	u2du000 2d20 (6%)
$^1A(6)$	3.92	22uu000 2dd0 (30%)	u22d000 2ud0 (23%)	2u2d000 2ud0 (16%)
$^1B(5)$	3.96	2udu000 2d20 (28%)	22u0000 2d20 (22%)	u2ud000 2d20 (9%)
$^1A(7)$	4.13	22uu000 2dd0 (53%)	2u2u000 2dd0 (27%)	u22u000 2dd0 (5%)
$^1B(6)$	4.24	2udu000 2d20 (36%)	2uud000 2d20 (26%)	ud2u000 2d20 (22%)
$^1A(8)$	4.40	u22u000 2dd0 (46%)	u22d000 2ud0 (42%)	2u2u000 2dd0 (3%)
$^1B(7)$	4.54	220u000 2d20 (35%)	u2du000 2d20 (20%)	222u000 2d00 (17%)
$^1B(8)$	4.60	220u000 2d20 (34%)	u2du000 2d20 (22%)	022u000 2d20 (21%)
$^1B(9)$	4.79	ud2u000 2d20 (40%)	uu2d000 2d20 (17%)	2udu000 2d20 (12%)
$^1A(9)$	4.87	2u2u000 2dd0 (53%)	u22u000 2dd0 (15%)	2u2d000 2ud0 (14%)
$^1B(10)$	4.98	222u000 2d00 (46%)	u2du000 2d20 25%)	022u000 2d20 (13%)
$^1A(10)$	5.24	2u2d000 2ud0 (43%)	u22d000 2ud0 (25%)	u22u000 2dd0 (12%)

[a] The MS-CASPT2 energies are in eV.

Apparently, only by choosing particular axial ligands will hemes bind small ligands, due to the decrease of spin splitting (ligand-field strength) induced by such ligands. This hypothesis was suggested in the case of dioxygen binding to heme.[32,33] This view of tetrapyrrole biochemistry implies that the design of axial ligands such as deprotonated and neutral histidine and cysteinate is toward lower spin splitting in hemes. In addition, this justifies the common sense that the metal orbitals must be tuned toward the tetrapyrrole frontier orbitals if any communication has to exist, as seen from simple perturbation theory. It is very interesting to observe that both in cob(I)alamin and in the widely different Fe[II] deoxyheme model, metal and ring orbitals interact by nondyncamical correlation, i.e., communicate.

For cob(I)alamin, the included π-LUMO is almost clean, without contributions from the metal, as seen in Figure 5. Instead, a covalent interaction between the corrin nitrogen orbitals and the $d_{x^2-y^2}$ orbital (MOs 44b and 46b) is found, which shows that nepheulauxetic effects complicate the simple ligand-field picture. Thus, in the case of cobalt(I) corrin, it is not the π-interactions, but instead σ-interactions, which provide communication between the tetrapyrrole ring and the metal. Pierloot[34] was the first to point out this important feature in iron(II) porphine, and apparently it seems to be a more general effect.

The detailed composition of the ground state is depicted in the first row of Table 3. The active space occupations are described by the 7 a and the 4 b orbitals, where 2 means doubly occupied, u means spin up, d means spin down, and 0 means unoccupied. In comparison with Figure 5, it is important to forget about the two highest inactive orbitals of each symmetry, 47a and 43b.

The most important configuration state function in the CI wave function is denoted CSF1. This configuration is the closed-shell (2220000 2200) d^8 configuration, making up 67% of the total correlated wave function. As already mentioned, it is not the native ligand-field d^8 configuration, although d_{z^2} is the lowest orbital, as expected, in the form of 48a and its 4d correlating partner, 52a. This is due to the fact that the optimized MOs are not pure atomic orbitals (AOs) but mixtures of ligand and metal AOs, although one type usually dominates. Notably, all five doubly occupied orbitals have some d-character, one of the $d_{xz,yz}$ orbitals has moved up in energy, and the 44b bonding orbital has become doubly occupied.

The second most important contribution is a significant (20%) metal-to-ligand charge-transfer (MLCT) excitation from 50a to 51a. This important contribution shows the rationale of including the LUMO of π-character into the active space, and it explains why DFT calculations[7] found an open-shell singlet ground state of cobalt(I) corrin. The third most important configuration is only 3% and is the corresponding MLCT excitation from 49a. Thus, it can be concluded that both DFT and CAS-SCF calculations agree on the multiconfigurational nature of cobalt(I) corrin insofar as a singlet instability point on the restricted Kohn−Sham potential energy surface can be taken as an indication of such a nature. At least, it shows in both methods the inadequacy of using the d^8 closed-shell formalism for cob(I)alamin, which has been invoked in all literature on cob(I)alam to date.[35]

Electronic Spectrum of Cobalt(I) Corrin. Now, the obtained electronic spectrum and the description of the excited states are discussed. For completion, both the singlet spectrum, depicted in Table 4, as well as the 20 lowest triplet states, depicted in Table 5, have been computed. The most important conclusion that shall be drawn from the triplet spectrum is that the lowest triplet state is 0.31 eV above the singlet ground state. Thus, CASPT2 predicts the correct spin state of the corrin complex, which is not always the case for porphyrin systems. Otherwise, this spectrum is reported here only for later reference, since it is not biologically relevant.

The transition moments obtained from the CAS self-interaction (SI) program of MOLCAS were used to compute the oscillator strengths f, as is done automatically by the program. The nonzero (dipole-allowed) transition matrix elements with the ground state are those involving the z-component for ^1A excited states and x- and y-components for ^1B excited states. The oscillator strengths are presented together with the excitation energies at various levels of theory in Table 4. They provide a rough estimate of the relative intensity of the various excited states and are thus used in the assignment of the important lines in the experimental spectrum. However, the oscillator strengths are not directly comparable with the line intensities because of broadening, vibrational progressions, coalescence, etc. However, they serve to identify the electronic excitations that are genuine to the spectrum, even though these may not be found by experiment. To reproduce the line form of the experimental

TABLE 4: Lowest Electronic States, Energies, and Oscillator Strengths with Respect to the Ground State for Cobalt(I) Corrin[a]

state	$E_{CAS-SCF}$ (eV)	E_{CASPT2} (eV)	$E_{MS-CASPT2}$ (eV)	$\lambda_{MS-CASPT2}$ (nm)	f_{CAS-SI}	λ_{EXP} (nm)	E_{EXP} (eV)	relative intensity$_{EXP}$
$^1A(2)$	0.35	0.69	1.14	1085	8.20E−004			
$^1B(1)$	**0.74**	**1.09**	**1.55**	**801**	**6.41E−002**	**800**	**1.55**	**(broad)**
$^1A(3)$	1.88	1.66	1.81	683	1.29E−003			
$^1A(4)$	**3.72**	**2.46**	**2.13**	**581**	**5.03E−003**	**554**	**2.24**	**0.13**
$^1B(2)$	**3.27**	**2.80**	**3.22**	**384**	**1.23E−002**	**385**	**3.22**	**1.0**
$^1B(3)$	3.52	2.90	3.28	378	2.00E−005			
$^1A(5)$	**3.83**	**1.73**	**3.36**	**369**	**1.32E+000**	**385**	**3.22**	**1.0**
$^1B(4)$	3.91	3.16	3.68	337	8.00E−005			
$^1A(6)$	**3.96**	**3.25**	**3.92**	**316**	**7.63E−001**	**300**	**4.13**	**0.9**
$^1B(5)$	3.93	3.61	3.96	313	1.99E−003			
$^1A(7)$	**4.24**	**3.57**	**4.13**	**300**	**1.96E−001**	**280/286**	**4.43/4.34**	**1.07/1.07**
$^1B(6)$	4.17	4.10	4.24	292	3.51E−006			
$^1A(8)$	4.28	3.94	4.40	282	1.90E−004			
$^1B(7)$	**4.35**	**3.73**	**4.54**	**273**	**6.24E−003**			
$^1B(8)$	4.59	4.13	4.60	269	3.00E−005			
$^1B(9)$	4.86	4.50	4.79	259	6.00E−005			
$^1A(9)$	**4.90**	**4.41**	**4.87**	**254**	**3.68E−003**			
$^1B(10)$	**4.94**	**4.27**	**4.98**	**249**	**5.07E−003**			
$^1A(10)$	**5.53**	**4.77**	**5.24**	**236**	**2.14E−001**			

[a] All energies are vertical, computed at the ground-state geometry. The states with the highest calculated intensities (used for assignment) are shown in bold.

TABLE 5: Lowest Triplet Electronic States and Energies with Respect to the Ground State for Cobalt(I) Corrin[a]

state	$E_{CAS-SCF}$ (eV)	E_{CASPT2} (eV)	$E_{MS-CASPT2}$ (eV)	$\lambda_{MS-CASPT2}$ (nm)
$^3A(1)$	0.31	0.91	1.35	921
$^3A(2)$	0.46	0.89	1.37	908
$^3A(3)$	1.05	0.99	1.42	871
$^3A(4)$	1.51	1.65	2.10	589
$^3A(5)$	1.92	2.01	2.46	505
$^3A(6)$	2.74	2.62	3.07	404
$^3A(7)$	3.75	3.38	3.81	326
$^3A(8)$	3.83	3.59	4.06	305
$^3A(9)$	4.15	4.09	4.29	289
$^3A(10)$	4.23	3.80	4.55	273
$^3B(1)$	0.73	1.09	1.37	906
$^3B(2)$	1.04	0.93	1.54	803
$^3B(3)$	1.65	1.69	2.08	596
$^3B(4)$	2.10	1.70	2.20	564
$^3B(5)$	3.42	2.51	2.80	443
$^3B(6)$	3.68	3.35	3.73	332
$^3B(7)$	3.78	3.31	3.86	321
$^3B(8)$	3.86	3.35	3.97	313
$^3B(9)$	4.15	4.10	4.35	285
$^3B(10)$	4.39	3.87	4.56	272

[a] All energies are vertical, computed at the ground-state geometry

spectrum, one needs to perform simulations that involve thermodynamics and solvation models, which is beyond the scope of this work.

From the five largest oscillator strengths ($f > 0.001$), five genuine states are found that would be expected to show up in the experimental spectrum. These include four high-intensity (>0.1) lines at 369, 236, 300, and 316 nm, together with medium-intensity (>0.1) states at 801 and 384 nm as well as some weak (>0.001) states at 581, 683, 313, 273, 254, and 249 nm. No states have been computed below 236 nm. The four most intense states can be assigned directly to four of the five most intense lines in the experimental spectrum,[36,37] so that experimental lines correspond to the following calculated states: 286 nm = $^1A(7)$ (wavelength 300 nm in this work), 300 nm = $^1A(6)$ (wavelength 316 nm in this work), 385 nm = $^1A(5)$ (and possibly $^1B(2)$) (wavelengths 369 and 384 nm in this work), and possibly 280 nm = $^1A(10)$ (wavelength 236 nm in this work). In addition, the $^1B(2)$ state is of large enough

intensity (the sixth largest in this work) for us to assume that it is part of the line at 385 nm.

The fifth largest intensity from the calculated spectrum is for the first excited state of B symmetry, $^1B(1)$, at 801 nm. This state is assigned to the broad 800 nm peak in the experimental spectrum, since this is the lowest energy excitation observed. The agreement in terms of energies for these six assignments is very good indeed, giving a root-mean-square error of 0.14 eV and largest error of 0.21 eV. The last state of significant intensity is not as well assigned, but it is concluded that it must be the $^1A(4)$ state, found at 554 nm in the experimental spectrum. With state $^1A(10)$ left unassigned, the assignment is in agreement with experiment to within 0.21 eV, as is expected for this approach. The $^1A(10)$ state is apparently too high in energy to occur in the experimental spectrum and is thus not observed.

Now, for a moment, the composition of the most important excited states according to the assignment in this work is discussed. First of all, Table 3 reveals a complex nature of many states. However, all the lowest states of A-symmetry, $^1A(1)$, $^1A(2)$, $^1A(3)$, and $^1A(4)$, consist mainly of single excitations from the ground-state CSF1, which is understandable since they are expected to have the lowest energies. The low-lying B-states usually involve double excitations: $^1B(1)$, $^1B(2)$, and $^1B(3)$. Of these, the most interesting ones are mentioned (i.e., the most intense ones). $^1B(1)$, the broad band at 800 nm, can be described as a double excitation out of 45b (which is of d_{xz}-type) to the porphyrin π-LUMO 51a and to the σ-antibonding orbital 46b. The notorious band at 385 nm is described by $^1B(2)$ as a double excitation out of the 49a (which is of d_{xy}-type) again to 51a and to 46b and accompanied by one further exciation from a d-orbital to 46b but is a highly multiconfigurational state (the weight of CSF1 is only 27%). The weaker line at 554 nm is assigned to $^1A(4)$, which is described as a one-electron MLCT excitation (51%) to the 51a. The other lines in the spectrum were assigned to $^1A(5)$, $^1A(6)$, and $^1A(7)$, which can be described as various double MLCT excitation simultaneously to 51a and 46b; as their natures are similar, so are their energies (286 nm, 300 nm, and 385 nm).

Comparison between DFT and MS-CASPT2. The double and triple excitations and charge-transfer excitations make the spectrum complicated and suggests that simpler theoretical

TABLE 6: Assignment from This Work Compared to the Nine TD-DFT States with Largest f from Ref 18 and with Experiment

CAS-SI state	$\lambda_{TD\text{-}DFT}$ (nm)	$\lambda_{MS\text{-}CASPT2}$ (nm)	λ_{EXP} (nm)	$f_{TD\text{-}DFT}$	$f_{CAS\text{-}SI}$	relative intensity$_{EXP}$
^{1}B(1)	786	801	800	1.30E−002	6.41E−002	(broad)
^{1}A(3)	617	581	554	2.40E−002	5.03E−003	0.13
^{1}B(2)	380	384	385	9.70E−002	1.23E−002	1.0
^{1}A(5)	350	369	385	2.40E−002	1.32E+000	1.0
	329			1.04E−001		
^{1}A(6)	319	316	300	8.80E−002	7.63E−001	0.9
^{1}A(7)	318	300	286	5.70E−002	1.96E−001	1.07
^{1}A(10)	312	236	280	4.30E−002	2.14E−001	
^{1}B(7)	303	273		4.30E−002	6.24E−003	

TABLE 7: Mulliken d-Orbital Occupations from the CAS-SCF Wave Functions

orbital	^{1}A(1)	^{1}A(2)	^{1}A(3)	^{1}A(4)	^{1}A(5)	^{1}A(6)	^{1}A(7)	^{1}A(8)	^{1}A(9)	^{1}A(10)
					state					
3d2+	1.77	1.34	1.75	1.77	1.73	1.37	1.87	1.15	1.85	1.78
3d2−	1.28	1.83	1.78	1.46	1.82	1.81	1.11	1.81	1.90	1.88
3d0	1.94	1.75	1.34	1.87	1.93	1.75	1.90	1.94	1.09	1.24
3d1−	1.87	1.89	1.75	1.19	1.64	1.07	1.09	1.01	1.02	1.01
3d1+	0.62	0.61	0.77	1.14	0.67	1.28	1.29	1.31	1.35	1.35
total d	7.47	7.42	7.42	7.42	7.79	7.28	7.26	7.23	7.21	7.26

orbital	^{1}B(1)	^{1}B(2)	^{1}B(3)	^{1}B(4)	^{1}B(5)	^{1}B(6)	^{1}B(7)	^{1}B(8)	^{1}B(9)	^{1}B(10)
					state					
3d2+	1.89	1.75	1.50	1.24	1.27	0.94	1.43	1.21	1.84	1.16
3d2−	1.92	1.28	1.31	1.39	1.10	1.73	1.16	1.55	1.86	1.11
3d0	1.96	1.00	1.44	1.42	1.66	1.58	1.46	1.29	1.25	1.80
3d1−	1.02	1.92	1.70	1.89	1.91	1.70	1.90	1.85	0.95	1.85
3d1+	0.59	1.34	1.32	1.34	1.32	1.31	1.34	1.35	1.33	1.36
total d	7.39	7.30	7.30	7.28	7.27	7.25	7.29	7.25	7.22	7.28

methods to reproduce the spectrum would fail. It is therefore interesting to compare the ab initio MS-CASPT2 spectrum with that obtained earlier by time-dependent density functional theory (TD-DFT), which used a Dunning DZP-type basis.[18] As is typical, there are many more states in the TD-DFT study but not many of significant intensity. Selecting the nine transitions with the largest oscillator strengths from that work,[18] a comparison as shown in Table 6 can be obtained. Since all the oscillator strengths of the TD-DFT study are similar, they cannot be used for assignment; this is of course a major drawback. That being said, the energies of the eight most intense lines in the DFT study are surprisingly close to the energies of the intense lines in the CASPT2 and experimental spectra. By ordering these eight excitations with decreasing wavelength, the DFT excitations can be assigned directly. With this approach, all states are better described by CASPT2 as expected. DFT describes a state at 329 nm, which is unaccounted for, and it is likely that this is a charge-transfer state. Since this is the most intense DFT excitation, it could be assigned to one of the other bands, thus lowering the accuracy of the DFT assignment further.

The conclusion is that CASPT2 is the more accurate method for obtaining the spectrum, as expected, and it reveals detailed information about the nature of the ground state and the excited states. However, the DFT method works reasonably well, considering the complex nature of the excited states, and it is fascinating that these two widely different methods can provide so similar results. Interestingly, in addition to the fully assigned spectra, both CASPT2 and DFT predict an extra peak at 273 nm (303 nm with DFT), with a medium to weak intensity.

Perspectives Regarding the Charge-Transfer Nature of the Cobalt(I) Corrin Ground State. It is reasonable to assume that cobalt(I) corrin is a very good model of cob(I)alamin, since

the effects of the cobalamin side chains are deemed very minor from earlier studies.[19] Since no axial ligands are supposed to bind cob(I)alamin in its active state, the vacuum model must be considered quite realistic (for determining the detailed shape of the spectrum though, one needs to account for more details, e.g., vibrational coupling). Thus, the conclusions that have been drawn regarding the ground state of cobalt(I) corrin are likely to have relevance for the true cobalamin cofactor.

To address in more detail the mixture of the Co^I and Co^{II} character in the cobalt(I) corrin wave function, the d-orbital occupations of the optimized CAS-SCF wave function have been computed from Mulliken population analysis. The results of such an analysis are presented in Table 7. The designation of the orbitals comply with the axis of inertia (the symmetry axis) used in the study, with the 3d^0 orbital aligned along this axis, and the other d-orbitals being components of ±1,2 on this axis. The important observations are that (i) very few d-orbitals have occupations close to 2, again confirming that the simple ligand-field picture is incorrect and (ii) the charge-transfer nature can be partly deduced from the d-occupation numbers, which lie in the interval from 7.2 to 7.8.

Although these numbers are far from accurate, the flaws of Mulliken population analysis being well-known, their *relative* sizes in the series indicates their charge-transfer nature. It has already been seen in the wave function analysis that most states have a Co^{II} nature due to MLCT excitations, in particular into the π-LUMO of the corrin ring. This also holds true for the ^{1}A(5) state, which exhibits the highest d-occupation of 7.79. All other states have lower d-occupations and thus apparently more charge-transfer character. Therefore, it can be said with some confidence that all the states have charge-transfer nature, as judged from both the wave function composition and the d-orbital occupations. It is interesting also to observe that all

of the low-lying excited states have similar d-orbital occupations, between 7.3 and 7.5, again suggesting some significance of the Mulliken analysis.

The observation that the ground state of cobalt(I) corrin is composed of at least 23% (CFS2 + 3) cobalt(II) configurations may have some biological significance. It is of interest to understand how the transferases stabilize the very uncommon Co[I] oxidation state. Obviously, these enzymes want a strong nucleophile for the ping pong reaction, but they are fighting against the redox chemistry of cobalt(I). The corrin ring, being monovalent, can in contrast to porphyrin rings provide part of the conditions for obtaining this monovalent state, as already discussed in detail elsewhere.[7] The cavity size of the corrin ring may also contribute to the accessibility of the Co[I] state.[7] However, a possible partial explanation emerging from this study is that the enzymes simply *do not have* to go all the way, breaking with the consensus of all in vitro redox chemistry. Instead, the cobalamin cofactor via its corrin ring facilitates the redox reaction by communicating directly with the ligand field, constituting a partial electron reservoir for the extra electron in the cofactor. Put another way, the cobalt ion is not the sole electron donor in the redox reaction; the corrin ring and the cobalt ion must be considered as a whole to understand the structure and function of the cob(I)alamin cofactor.

References and Notes

(1) Ludwig, M. L.; Matthews, R. G. *Annu. Rev. Biochem.* **1997**, *66*, 269.

(2) Wirt, M. D.; Sagi, I.; Chance, M. R. *Biophys. J.* **1992**, *63*, 412.

(3) Wirt, M. D.; Sagi, I.; Chen, E.; Frisbie, S. M.; Lee, R.; Chance, M. R. *J. Am. Chem. Soc.* **1991**, *113*, 5299.

(4) Banerjee, R. V.; Frasca, V.; Ballou, D. P.; Matthews, R. G. *Biochemistry* **1990**, *29*, 11101.

(5) Jensen, K. P.; Ryde, U. *J. Am. Chem. Soc.* **2003**, *125*, 13970.

(6) Schrauzer, G. N.; Deutsch, E.; Wingassen, R. J. *J. Am. Chem. Soc.* **1968**, *90*, 241.

(7) Jensen, K. P.; Ryde, U. *ChemBioChem* **2003**, *4*, 413.

(8) Dölker, N.; Maseras, F. *J. Phys. Chem. B* **2001**, *105*, 7564.

(9) Jensen, K. P.; Sauer, S. P. A.; Liljefors, T.; Norrby, P.-O. *Organometallics* **2001**, *20*, 550.

(10) Andruinow, T.; Zgierski, M. Z.; Kozlowski, P. M. *J. Phys. Chem. A* **2002**, *106*, 1365.

(11) Jensen, K. P.; Ryde, U. *THEOCHEM* **2002**, *585*, 239.

(12) Andruniow, T.; Zgierski, M. Z.; Kozlowski, P. M. *J. Phys. Chem. B* **2000**, *104*, 10921.

(13) Andruniow, T.; Zgierski, M. Z.; Kozlowski, P. M. *J. Am. Chem. Soc.* **2001**, *123*, 2679.

(14) Jensen, K. P.; Ryde, U. *J. Phys. Chem. B* **2003**, *107*, 7539.

(15) Ouyang, L.; Randaccio, L.; Rulis, P.; Kurmaev, E. Z.; Moewes, A.; Ching, W. Y. *THEOCHEM* **2003**, *622*, 221.

(16) Stich, T. A.; Brooks, A. J.; Buan, N. R.; Brunold, T. C. *J. Am. Chem. Soc.* **2003**, *125*, 5897.

(17) Andruinow, T.; Kozlowski, P. M.; Zgierski, M. Z. *J. Chem. Phys.* **2002**, *115*, 7522.

(18) Jaworska, M.; Kazibut, G.; Lodowski, P. *J. Phys. Chem. A* **2003**, *107*, 1339.

(19) Jensen, K. P.; Mikkelsen, K. V. *Inorg. Chim. Acta* **2001**, *323*, 5.

(20) Schäfer, A.; Horn, H.; Ahlrichs, R. *J. Chem. Phys.* **1992**, *97*, 2571.

(21) Alrichs, R.; Bär, M.; Häser, M.; Horn, H.; Kölmel, C. *Chem. Phys. Lett.* **1989**, *162*, 165.

(22) Andersson, K.; Barysz, M.; Bernhardsson, A.; Blomberg, M. R.A.; Carissan, Y.; Cooper, D. L.; Fleig, T.; Fulscher, M. P.; Gagliardi, L.; de Graaf, C.; Hess, B. A.; Karlstrom, G.; Lindh, R.; Malmqvist, P.-A.; Neogrdy, P.; Olsen, J.; Roos, B. O.; Schimmelpfennig, B.; Schtz, M.; Seijo, L.; Serrano-Andrs, L.; Siegbahn, P. E. M.; Stahlring, J.; Thorsteinsson, T.; Veryazov, V.; Wierzbowska, M.; Widmark, P.-O. *MOLCAS*, version 5.4; Department of Theoretical Chemistry, Lund University: Lund, Sweden, 2002.

(23) Andersson, K.; Malmqvist, P.-A.; Roos, B. O.; Sadlej, A. J.; Wolinski, K. *J. Phys. Chem.* **1990**, *94*, 5483.

(24) Andersson, K.; Malmqvist, P.-A.; Roos, B. O. *J. Chem. Phys.* **1992**, *96*, 1218.

(25) Roos, B. O.; Andersson, K.; Fulscher, M. P.; Malmqvist, P.-A.; Serrano-Andrs, L.; Pierloot, K.; Merchn, M. In *New Methods in Computational Quantum Mechanics*; Advances in Chemical Physics 93; Prigogine, I., Rice, S. A., Eds.; John Wiley & Sons: New York, 1996.

(26) Widmark, P.-O.; Malmqvist, P.-A.; Roos, B. O. *Theor. Chim. Acta* **1990**, *77*, 291.

(27) Roos, B. O.; Taylor, P. R.; Siegbahn, P. E. M. *Chem. Phys.* **1980**, *48*, 157.

(28) Finley, F.; Malmqvist, P.-A.; Roos, B. O.; Serrano-Andrs, L. *Chem. Phys. Lett.* **1997**, *288*, 299.

(29) Roos, B. O.; Andersson, K.; Fulscher, M. P.; Serrano-Andrs, L.; Pierloot, K.; Merchn, M.; Molina, V. *THEOCHEM* **1996**, *388*, 257.

(30) Jensen, K. P.; Roos, B. O.; Ryde, U. *J. Inorg. Biochem.* **2005**, *99*, 45.

(31) Gouterman, M. *J. Chem. Phys.* **1959**, *30*, 1139.

(32) Jensen, K. P.; Ryde, U. *J. Biol. Chem.* **2004**, *279*, 14561.

(33) Jensen, K. P.; Ryde, U. *Mol. Phys.* **2003**, *101*, 2003.

(34) Pierloot, K. *Mol. Phys.* **2003**, *101*, 2083.

(35) Matthews, R. G. *Acc. Chem. Res.* **2001**, *34*, 681.

(36) Boos, R. N.; Carr, J. E.; Conn, J. B. *Science* **1953**, *117*, 603.

(37) Tackett, S. L.; Collat, J. W.; Abbott, J. B. *Biochemistry* **1963**, *2*, 919.